

Magnetic susceptibility and spin-glass transition in $\text{Zn}_{1-x}\text{Mn}_x\text{Te}$

S. P. McAlister

Division of Chemistry, National Research Council of Canada, Ottawa K1A 0R9, Canada

J. K. Furdyna

Department of Physics, Purdue University, West Lafayette, Indiana 47907

W. Giriat

Centro de Física, Instituto Venezolano de Investigaciones Científicas, Apartado 1827, Caracas 1010A, Venezuela

(Received 6 June 1983)

Magnetic susceptibility of the diluted magnetic semiconductor $\text{Zn}_{1-x}\text{Mn}_x\text{Te}$ was studied between 2 and 250 K for the Mn concentration range $0.15 < x < 0.70$. When $x > 0.20$, this zinc-blende ternary system exhibits a spin-glass transition at low temperatures, as evidenced by a cusp in the susceptibility and by the presence of irreversible effects. Because $\text{Zn}_{1-x}\text{Mn}_x\text{Te}$ is an insulator, and the interactions between the Mn ions are antiferromagnetic, the observed spin-glass behavior is attributed to frustration inherent in the fcc sublattice partially occupied by Mn. For the same value of x , the transition temperatures for $\text{Zn}_{1-x}\text{Mn}_x\text{Te}$ are consistently higher than those observed in the closely related zinc-blende compound $\text{Cd}_{1-x}\text{Mn}_x\text{Te}$. From this we infer that the value of the exchange integral is higher in $\text{Zn}_{1-x}\text{Mn}_x\text{Te}$.

I. INTRODUCTION

The ternary compound $\text{Zn}_{1-x}\text{Mn}_x\text{Te}$ belongs to a family of materials known as diluted magnetic semiconductors (DMS's), sometimes also referred to as "semimagnetic" semiconductors. These materials have recently been the subject of extensive studies because of their important semiconducting as well as magnetic properties.¹ This ternary system crystallizes in the zinc-blende structure in the composition range $x \leq 0.80$, the Mn^{2+} ions replacing Zn^{2+} at random lattice sites.² Since MnTe itself crystallizes in the NiAs structure, the incompatibility of the latter crystal lattice with the zinc-blende phase imposes an upper limit on x .

The presence of substitutional Mn^{2+} ions is responsible for the magnetic properties of DMS's. These properties are important in their own right,³ providing insights into the behavior of a random magnetic system, such as the spin-glass transition in a frustrated fcc lattice, formation of antiferromagnetic clusters, etc. Moreover, knowledge of the magnetization of the Mn subsystem in DMS's is important in that it bears on the optical and electronic properties of DMS's through the spin-spin exchange interaction between the localized moments and band electrons,^{1,4} leading to entirely novel effects, e.g., a large, temperature-dependent g factor, gigantic Faraday rotation, etc.

In this paper we have undertaken a systematic study of the magnetic properties of $\text{Zn}_{1-x}\text{Mn}_x\text{Te}$ over a broad composition range. This study has long been overdue inasmuch as considerable effort has already been expended on the study of the magnetic structure of $\text{Zn}_{1-x}\text{Mn}_x\text{Te}$ by neutron diffraction,^{5,6} and measurements of dc magnetization are needed for a better understanding of the neutron

data. Furthermore, magnetic susceptibility studies of $\text{Zn}_{1-x}\text{Mn}_x\text{Te}$ afford an opportunity to compare its susceptibility parameters with those of $\text{Cd}_{1-x}\text{Mn}_x\text{Te}$, which has an identical crystal structure, but at any given value of x differs from the former by the Mn-Mn separation.

II. EXPERIMENT

The samples of $\text{Zn}_{1-x}\text{Mn}_x\text{Te}$ used in this study were prepared either by Bridgman growth or by sintering, using, in both instances, individual elements as starting materials. The composition was characterized by determining the lattice parameter a_0 of each specimen, and using the known dependence of a_0 on x to obtain the composition.⁷ The lattice parameter was determined at room temperature by x-ray powder diffraction, using a Guinier camera and the $K\alpha_1$ line of copper ($\lambda = 1.5406 \text{ \AA}$), with Si as an internal standard. The powder samples were taken from the immediate vicinity (within a millimeter or so) of the specimen used in the susceptibility measurements to avoid uncertainty due to possible composition gradients.

The susceptibility and magnetization experiments were performed using a vibrating-sample magnetometer with fields ranging up to 2 T and temperatures between 2 and 300 K. Absolute values were obtained by calibration with respect to 5N Ni.

III. RESULTS

As in other DMS's, the most striking feature in the behavior of $\text{Zn}_{1-x}\text{Mn}_x\text{Te}$ is the spin-glass transition, as evidenced by the characteristic cusp observed in the zero-field-cooled magnetic susceptibility. This is illustrated by Fig. 1, showing dc susceptibility data for a sample with

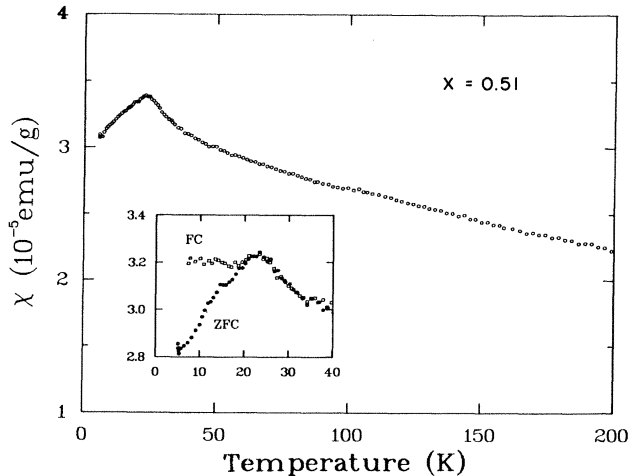


FIG. 1. ZFC dc magnetic susceptibility for the temperature range 4.2–200 K for $\text{Zn}_{1-x}\text{Mn}_x\text{Te}$ ($x=0.51$). The measuring field was 500 Oe. Note the susceptibility cusp, indicating T_0 . In the inset we also compare ZFC and FC data in an expanded scale near T_0 , showing the presence of irreversible effects below the cusp temperature.

$x=0.51$. The figure shows the temperature dependence of zero-field-cooled susceptibility over the range from 4.2 to 200 K, with a well-defined cusp at 23 K. The susceptibility was measured using a field of 500 Oe.

The identification of the cusp as a spin-glass transition is further supported by the existence of irreversible effects taking place below the cusp temperature T_0 . Typical data illustrating this feature for the $x=0.51$ sample are shown in the inset of Fig. 1. Here the data labeled “ZFC” (zero-field cooled) represent the susceptibility χ measured after first cooling the sample in zero magnetic field to 4.2 K, and then applying the field of 500 Oe. The data marked “FC” (field cooled) corresponds to values of χ obtained when the sample was cooled in the applied field.

Similar irreversible effects are illustrated in Fig. 2 for a

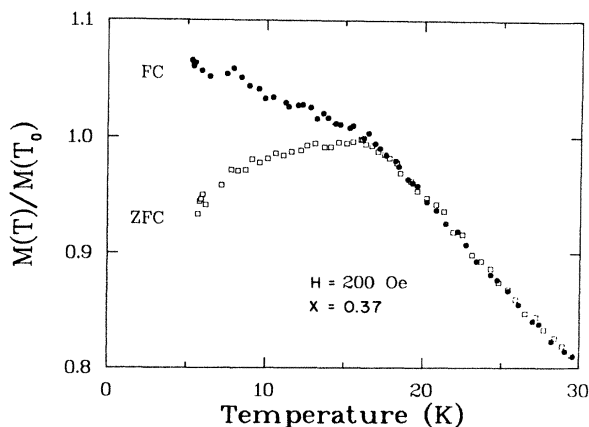


FIG. 2. Comparison of FC and ZFC magnetizations for $\text{Zn}_{1-x}\text{Mn}_x\text{Te}$ with $x=0.37$, measured in 200 Oe. The values of magnetization are normalized by its value at T_0 . Irreversible effects are clearly present below T_0 .

sample of $\text{Zn}_{1-x}\text{Mn}_x\text{Te}$ with $x=0.37$, showing the temperature dependence of field-cooled and zero-field-cooled magnetization, normalized by its value at the cusp temperature ($T_0 \approx 16.5$ K).

Although in the $x=0.37$ sample the cusp is somewhat rounded (possibly due to small local fluctuations in the value of x about an average value), the difference between field-cooled and zero-field-cooled data shown in Figs. 1 and 2 constitutes an unmistakable signature of irreversible behavior characteristic of spin-glasses. As in previous low-temperature studies of other insulating DMS's,^{1,3,8–10} the existence of a spin-glass phase in $\text{Zn}_{1-x}\text{Mn}_x\text{Te}$ is attributed to lattice frustration. This is consistent with the prediction of DeSeze,¹¹ who showed that in insulating materials where antiferromagnetically interacting magnetic moments occupy random sites on an fcc sublattice (as do the Mn^{2+} ions in $\text{Zn}_{1-x}\text{Mn}_x\text{Te}$), the system will undergo a spin-glass transition as a result of frustration.

Figure 3 illustrates the rather spectacular difference in the magnetic behavior of $\text{Zn}_{1-x}\text{Mn}_x\text{Te}$ samples with low ($x=0.33$) and high ($x=0.70$) concentrations. The magnetizations (field-cooled) are normalized by their values at the respective transition temperatures, with $M(T)/M(T_0)$ for the $x=0.70$ sample shifted downward (by multiplying by 0.9) to avoid obscuring the lower- x data near T_0 . The $x=0.70$ magnetization appears rather featureless, but shows a weak reproducible maximum about 42–43 K, which we identify as T_0 for that value of x . Furthermore, the $x=0.70$ data showed no difference between field-cooled and zero-field-cooled magnetizations below T_0 . While irreversible effects cannot be entirely ruled out in this range of x , their presence remained below noise level of our measurements, further emphasizing the large difference in the character of magnetization at high and low x .

Comparison of the data for $x=0.33$, 0.37, and 0.51

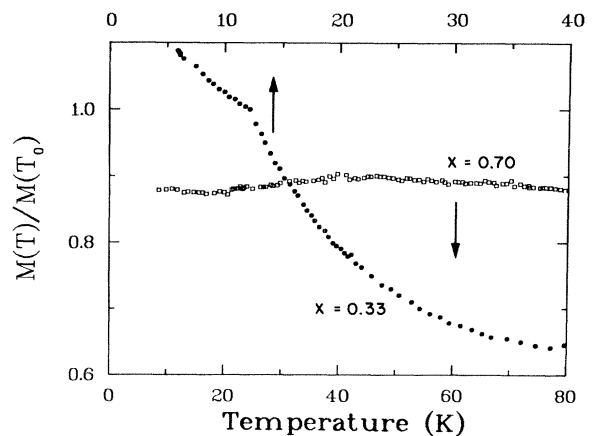


FIG. 3. Comparison of the temperature dependence of FC magnetization $M(T)$ for $\text{Zn}_{1-x}\text{Mn}_x\text{Te}$ with high and low values of x . Values of $M(T)$ have been normalized by values of $M(T_0)$ corresponding to each set of data, and the data for $x=0.70$ have been shifted downward for clarity. In the case of the $x=0.70$, no difference between FC and ZFC data is observed.

(Figs. 3, 2, and 1, respectively) reveals that the relative sharpness of the cusp is best defined for the $x=0.51$ sample, while for $x=0.33$ the magnetic susceptibility continues to increase even below T_0 . This is probably caused by loose spins, which may be present below T_0 , as suggested by Escorne and Mauger¹² in their studies of $\text{Cd}_{1-x}\text{Mn}_x\text{Te}$ in a similar range of x . The background of such loose spins would continue to contribute an additive Curie-Weiss-type term even below T_0 , which will result in an additive partial susceptibility that would increase with decreasing temperature. It appears logical that the relative population of such loose spins would be greater for more magnetically dilute samples. The argument for the existence of loose spins is further corroborated by the behavior of field-cooled data. In classical spin-glasses, such as CuMn , the field-cooled magnetization below T_0 either decreases or stays flat, whereas in our data it continues to increase below T_0 for samples with $x < 0.50$. Such behavior would be expected if a fraction of the spins remained "loose," i.e., capable of a Curie-Weiss behavior.

Figure 4 shows a typical behavior of field-cooled χ (inset) and χ^{-1} as a function of temperature for a sample with $x=0.37$, measured at 1 kOe. The inset shows χ on an expanded scale in the immediate vicinity of T_0 . The higher magnetic field leads to a rounding off of the field-cooled "knee," but otherwise the data is identical to the field-cooled magnetization obtained on the same sample at much lower fields, shown in Fig. 2.

Two features worthy of note are apparent at $T > T_0$ in Fig. 4. The high-field portion indicates clear Curie-Weiss behavior, providing a reliable measure of the Curie-Weiss temperature Θ . Below about 50 K one also observes a characteristic downturn of the χ^{-1} curve from the behavior predicted by extrapolating the Curie-Weiss law to low temperatures. Such "enhanced paramagnetism" is observed^{8-10,12} in all DMS's above T_0 , and suggests the

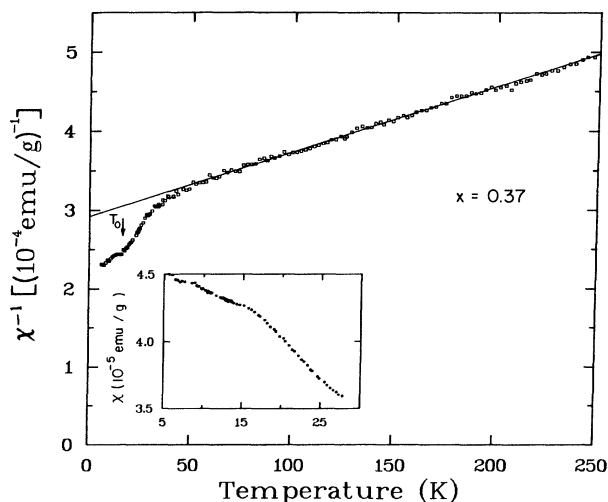


FIG. 4. FC χ (inset) and χ^{-1} for $x=0.37$ for a broad temperature range, observed in an applied field of 1 kOe. Note the excellent Curie-Weiss behavior above $T \approx 50$ K and a characteristic downturn of χ^{-1} observed below this temperature, but above T_0 .

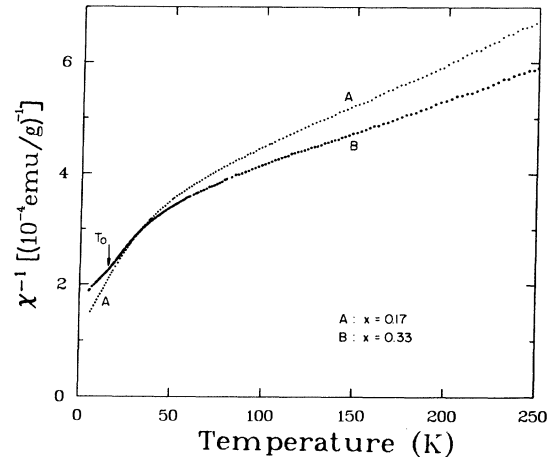


FIG. 5. Inverse susceptibility χ^{-1} vs T for two low-concentration samples, one of which is below the percolation limit and does not exhibit T_0 .

possibility of random cluster formation. This behavior is illustrated for two other samples in Fig. 5, showing that the characteristic downturn occurs whether a spin-glass transition is observed or not.

It should be mentioned parenthetically that in the closely related compound $\text{Cd}_{1-x}\text{Mn}_x\text{Te}$ remanent effects were reported to persist even above T_0 (at least for samples with $x \approx 0.3$), and this has been used to further support the inference that antiferromagnetically coordinated clusters survive considerably above the freezing temperature.¹² A qualitatively similar behavior should, in principle, be expected for $\text{Zn}_{1-x}\text{Mn}_x\text{Te}$. In our experiments, however, we have not observed explicit irreversible effects in the region $T > T_0$, as can be seen by the merging of FC and ZFC curves in Figs. 1 and 2. This may be because the effects or remanence above T_0 are less than our experimental error. Note also that the effects reported in Ref. 12 were observed at considerably lower temperatures than we used. It is possible that they are particularly strong below 4 K, while we have concentrated on samples with $T_0 > 10$ K. Future experiments on $\text{Zn}_{1-x}\text{Mn}_x\text{Te}$, performed on samples with $x \approx 0.2-0.25$ (where $T_0 < 4$ K), may thus also reveal traces of remanence at $T > T_0$ in this material. In any event, it would be premature at this point to use the absence of irreversible effects above T_0 in our data as an indication of significant differences between the magnetic behavior of $\text{Zn}_{1-x}\text{Mn}_x\text{Te}$ and $\text{Cd}_{1-x}\text{Mn}_x\text{Te}$.

Figure 6 shows a calculation of the effective number of Bohr magnetons P per Mn^{2+} ion as a function of T for two concentrations, calculated using the Curie-Weiss form for the susceptibility. Writing the effective moment μ as $\mu = P\mu_B$, we have

$$\frac{d\chi^{-1}}{dT} = \frac{3k_B}{NP^2\mu_B^2}, \quad (1)$$

where N is the number of moments per unit volume and χ is the volume susceptibility. Hence,

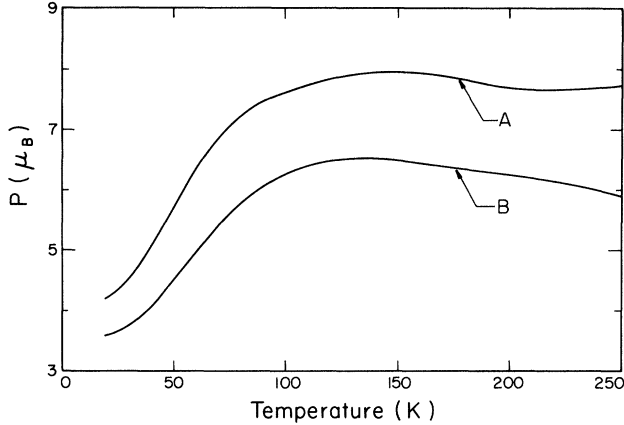


FIG. 6. Temperature dependence of the effective moment P obtained from $(d\chi^{-1}/dT)^{-1/2}$ (see text) for $x=0.17$ (A) and $x=0.33$ (B). The curves are obtained from fits to the original susceptibility data.

$$P = \left(\frac{3k_B}{N\mu_B^2} \right)^{1/2} \left(\frac{d\chi^{-1}}{dT} \right)^{-1/2} \quad (2)$$

The value of N for each sample is obtained from the measured value of the mole fraction x . The results in Fig. 6 are somewhat surprising in that at high temperatures both samples show an effective number of Bohr magnetons per Mn ion that is considerably higher than the value of $5\mu_B$ corresponding to free Mn ions. We have no explanation for these results at the present time, and report them only in an empirical spirit. It would not be particularly meaningful to speculate on the physical origins of the large values of P without having a microscopic theoretical model for the magnetic susceptibility of diluted magnetic semiconductors such as $\text{Zn}_{1-x}\text{Mn}_x\text{Te}$. However, the above results should provide one more reason why developing such a model would be important and timely, even for the (presumably) simpler high-temperature region corresponding to the Curie-Weiss limit.

In Fig. 7 we plot the Curie-Weiss temperature Θ for $\text{Zn}_{1-x}\text{Mn}_x\text{Te}$ obtained by extrapolating the linear, high-temperature behavior of χ^{-1} vs T . The values of Θ for higher x are somewhat less reliable because there χ^{-1} is rather flat and the extrapolation less certain. The solid curve is merely a guide for the eye. These values of Θ are remarkably large, as is the case for other DMS's studied earlier.

It is interesting to compare quantitatively the constants Θ for $\text{Zn}_{1-x}\text{Mn}_x\text{Te}$ with those obtained for $\text{Cd}_{1-x}\text{Mn}_x\text{Te}$ at the same Mn concentration. We show Θ vs x for $\text{Cd}_{1-x}\text{Mn}_x\text{Te}$, taken from Oseroff,¹⁰ by the dashed curve. Note that for any given x the $\text{Cd}_{1-x}\text{Mn}_x\text{Te}$ values are decidedly less than those for $\text{Zn}_{1-x}\text{Mn}_x\text{Te}$. We recall that the ionic radius of Cd^{2+} is 0.97 \AA and that of Zn^{2+} is 0.74 \AA . Also, the lattice parameter of $\text{Zn}_{1-x}\text{Mn}_x\text{Te}$ is considerably smaller than that of $\text{Cd}_{1-x}\text{Mn}_x\text{Te}$.⁷ Now the exchange interaction between two Mn spins S_i and S_j ,

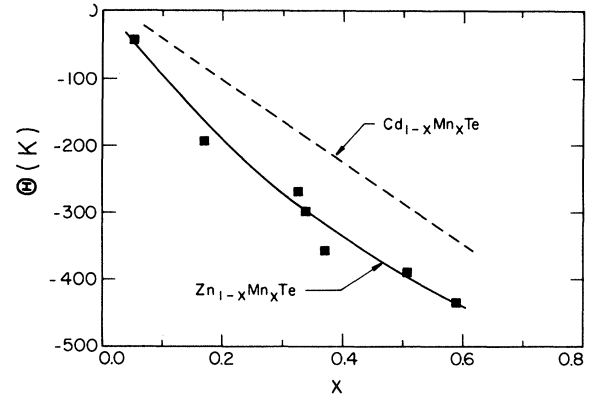


FIG. 7. Curie-Weiss temperature Θ as a function of x for $\text{Zn}_{1-x}\text{Mn}_x\text{Te}$, obtained from extrapolating the high-temperature linear behavior of $\chi^{-1}(T)$. The solid line is merely a guide for the eye. For comparison, the dashed line shows Θ vs x for the sister compound $\text{Cd}_{1-x}\text{Mn}_x\text{Te}$, taken from Ref. 10.

which is responsible for the finite value of Θ , can be written in the Heisenberg form

$$U = -2J\vec{S}_i \cdot \vec{S}_j, \quad (3)$$

where J is the exchange integral reflecting the overlap of the charge distributions of the spins S_i and S_j . Since the Mn-Mn distance is smaller in $\text{Zn}_{1-x}\text{Mn}_x\text{Te}$ than in $\text{Cd}_{1-x}\text{Mn}_x\text{Te}$, the exchange integral for the former is expected to be larger, and perhaps the relative behavior of Θ in the two compounds should not be surprising.

Finally, we show in Fig. 8 a magnetic phase diagram for $\text{Zn}_{1-x}\text{Mn}_x\text{Te}$, i.e., a locus of T_0 as a function of x , separating the paramagnetic (P) and spin-glass (SG) regions. The points are experimental, and the solid curve is merely a guide for the eye. It is to be emphasized that the diagram is drawn only on the basis of the observed T_0 in magnetization measurements. Uncertainties still exist as

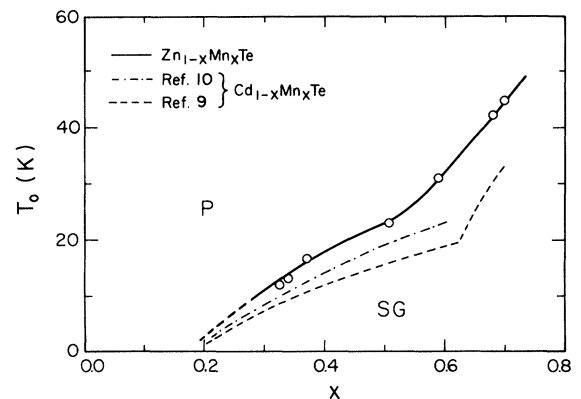


FIG. 8. Magnetic phase diagram for $\text{Zn}_{1-x}\text{Mn}_x\text{Te}$, separating the P and SG phases. The points correspond to the observed cusp temperature T_0 , and the solid curve is only a guide for the eye. Also shown are the phase diagrams reported for $\text{Cd}_{1-x}\text{Mn}_x\text{Te}$ in Refs. 9 (dashed line) and 10 (dashed-dotted line).

to the exact nature of the spin-glass phase in DMS's.¹²

It is again interesting to compare the magnetic phase diagram for $Zn_{1-x}Mn_xTe$ with that observed for $Cd_{1-x}Mn_xTe$, which crystallizes in the same zinc-blende structure over a comparable range of x . We have plotted in Fig. 8 the $Cd_{1-x}Mn_xTe$ phase diagrams reported by Galazka *et al.*⁹ (dashed line) and Oseroff¹⁰ (dashed-dotted line). The transition temperature differs somewhat between these two authors, but it is important to note that both give T_0 for $Cd_{1-x}Mn_xTe$ that is lower than the value for $Zn_{1-x}Mn_xTe$ for the same Mn concentration. This observation is again consistent with a higher value of the exchange integral which is expected for $Zn_{1-x}Mn_xTe$ on the grounds discussed above. Because of stronger Mn-Mn interaction in this compound, it is reasonable to expect the spin-glass freezing to occur at a higher temperature. A similar difference, consistent with qualitatively similar arguments, has recently been observed¹³ in the magnetic phase diagrams of the two wurtzite DMS's, $Cd_{1-x}Mn_xS$ and $Zn_{1-x}Mn_xS$.

While the value of T_0 for any x above the percolation threshold may depend on the details of composition of a specific ternary alloy, the percolation threshold itself (the lower limit on x for the onset of the spin-glass behavior) is dictated by the topology of the fcc lattice as such, independent of the specific ionic radii, lattice parameters, etc. It is important to note, then, that our experimental points in Fig. 8 extrapolate to approximately the same critical value of x at $T=0$ as do the $Cd_{1-x}Mn_xTe$ data.

In summary, we have shown that the magnetic behavior of the ternary DMS alloy $Zn_{1-x}Mn_xTe$ is essentially very

close to that of other DMS compounds studied so far. For low values of x the system is paramagnetic, exhibiting at high temperatures a strictly linear Curie-Weiss behavior indicative of antiferromagnetic Mn-Mn interaction, and an "enhanced paramagnetic" downturn of the χ^{-1} -vs- T curve at low temperatures, which has been ascribed to the formation of local spin clusters. Above $x \approx 0.20$, $Zn_{1-x}Mn_xTe$ exhibits a low-temperature spin-glass phase associated with frustration of the fcc lattice. Finally, the magnitudes of the Curie-Weiss temperatures Θ and the values of the spin-glass transition temperatures T_0 are higher at any given x in $Zn_{1-x}Mn_xTe$ than in the sister compound $Cd_{1-x}Mn_xTe$, which is identical to the former in every respect except in the lattice parameter and the ionic radius of the cation. From this we infer that the exchange integral is higher in $Zn_{1-x}Mn_xTe$.

ACKNOWLEDGMENTS

The authors wish to thank C. M. Hurd for his continued interest and useful discussions throughout this research. One of us (J.K.F.) would like to express his gratitude to the Division of Chemistry of the National Research Council of Canada, whose hospitality he enjoyed while most of this work was carried out. Finally, we thank the Purdue University Central Materials Preparation Facility, supported by the National Science Foundation Materials Research Laboratory program No. DMR-80-20249, for some of the crystals used in this investigation.

¹J. K. Furdyna, *J. Appl. Phys.* **53**, 7637 (1982).

²A. Pajczkowska, *Prog. Cryst. Growth Charact.* **1**, 289 (1978).

³R. R. Galazka, in *Proceedings of the International Conference on the Physics of Narrow Gap Semiconductors, Linz, 1981*, No. 152 of *Lecture Notes in Physics*, edited by E. Gornik, H. Heinrich, and L. Palmetshofer (Springer, Berlin, 1982), p. 294.

⁴J. Mycielski, *Recent Developments in Condensed Matter Physics*, edited by J. T. Devreese (Plenum, New York, 1981), Vol. I, p. 725.

⁵T. M. Holden, G. Dolling, V. F. Sears, J. K. Furdyna, and W. Girit, *Phys. Rev. B* **26**, 5074 (1982).

⁶G. Dolling, T. M. Holden, V. F. Sears, J. K. Furdyna, and W. Girit, *J. Appl. Phys.* **53**, 7644 (1982).

⁷J. K. Furdyna, W. Girit, D. F. Mitchell, and G. I. Sproule, *J. Solid State Chem.* **46**, 349 (1983).

⁸S. Nagata, R. R. Galazka, D. P. Mullin, H. Akbarzadeh, G. H. Khattak, J. K. Furdyna, and P. H. Keesom, *Phys. Rev. B* **22**, 3331 (1980).

⁹R. R. Galazka, S. Nagata, and P. H. Keesom, *Phys. Rev. B* **22**, 3344 (1980).

¹⁰S. B. Oseroff, *Phys. Rev. B* **25**, 6584 (1982).

¹¹L. DeSeze, *J. Phys. C* **10**, L353 (1977).

¹²M. Escorne and A. Mauger, *Phys. Rev. B* **25**, 4674 (1982).

¹³Y. Q. Yang, P. H. Keesom, J. K. Furdyna, and W. Girit, *J. Solid State Chem.* **49**, 20 (1983).